Western Pacific oceanic heat content: a better predictor of La Niña than of El Niño

Geophysical Research Letters

RESEARCH LETTER
10.1029/2018GL079341

Key Points:
- The western equatorial Pacific heat content is the best El Niño-Southern Oscillation oceanic predictor beyond 1-year lead
- This relation is asymmetrical: La Niña amplitude and occurrence is more predictable than that of El Niño
- Weak western Pacific heat content recharges, stronger air-sea coupling, and atmospheric stochasticity contribute to this asymmetry

Supporting Information:
- Supporting Information S1

Correspondence to:
Y. Planton,
yann.planton@gmail.com

Citation:
Planton, Y., Vialard, J., Guilyardi, E., Lengaigne, M., & Izumo, T. (2018). Western Pacific oceanic heat content: A better predictor of La Niña than of El Niño. *Geophysical Research Letters*, *45*. https://doi.org/10.1029/2018GL079341

Received 22 JUN 2018
Accepted 20 AUG 2018
Accepted article online 27 AUG 2018

Western Pacific Oceanic Heat Content: A Better Predictor of La Niña Than of El Niño

Yann Planton[1], Jérôme Vialard[1], Eric Guilyardi[1,2], Matthieu Lengaigne[1,3], and Takeshi Izumo[1,3]

[1]LOCEAN-IPSL (Sorbonne Université-CNRS-IRD-MNHN), Paris, France, [2]NCAS-Climate, University of Reading, Reading, UK, [3]Indo-French Cell for Water Sciences, IISc-NIO-IITM–IRD Joint International Laboratory, NIO, Dona Paula, India

Abstract The western equatorial Pacific oceanic heat content (warm water volume in the west or WWV_w) is the best El Niño–Southern Oscillation (ENSO) predictor beyond 1-year lead. Using observations and selected Coupled Model Intercomparison Project Phase 5 simulations, we show that a discharged WWV_w in boreal fall is a better predictor of La Niña than a recharged WWV_w for El Niño 13 months later, both in terms of occurrence and amplitude. These results are robust when considering the heat content across the entire equatorial Pacific (WWV) at shorter lead times, including all Coupled Model Intercomparison Project Phase 5 models or excluding Niño-Niña and Niña-Niño phase transitions. Suggested mechanisms for this asymmetry include (1) the negatively skewed WWV_w distribution with stronger discharges related to stronger wind stress anomalies during El Niño and (2) the stronger positive Bjerknes feedback loop during El Niño. The possible role of stronger subseasonal wind variations during El Niño is also discussed.

Plain language summary El Niño and La Niña have strong societal impacts at the global scale, especially large-amplitude El Niño events like in 1982–1983, 1997–1998, and 2015–2016. It is hence important to identify early warning signals for the occurrence of El Niño/La Niña. The equatorial Pacific Ocean heat content is a well-known predictor of El Niño/La Niña several seasons ahead. In this study, we show that negative heat content anomalies lead more systematically to La Niña events than positive heat content to El Niño events. We suggest that the enhanced predictability of La Niña relative to El Niño is due to larger negative heat content anomalies ahead of La Niña events and a more unstable (and hence less predictable) ocean-atmosphere system during El Niño.

1. Introduction

The El Niño–Southern Oscillation (ENSO) is the dominant source of interannual climate variability, with large environmental and socioeconomic impacts at global scale (McPhaden, Zebiak, et al., 2006). El Niño (La Niña), the positive (negative) phase of ENSO, is characterized by anomalously warm (cold) surface and subsurface temperatures in the central and eastern equatorial Pacific, associated with anomalously weak (strong) trade winds. Sometimes, El Niño can be exceptionally large, as in 1982, 1997, and 2015, with sea surface temperature anomalies (SSTAs) exceeding 3 °C in the eastern equatorial Pacific. These extreme events have strong impacts on, for example, tropical cyclones, marine and terrestrial ecosystems, and agriculture worldwide (Cai et al., 2014; McPhaden, Zebiak, et al., 2006; Santoso et al., 2017). It is hence of utmost importance to reliably forecast the occurrence and amplitude of ENSO, in particular extreme events.

The equatorial Pacific heat content is a long-lead ENSO precursor (Meinen & McPhaden, 2000; Wyrtki, 1985; Zebiak & Cane, 1987), underlining the role of the oceanic state for ENSO predictability. This has motivated the development of skillful ENSO forecasts by coupled ocean-atmosphere models, up to three seasons before its peak (e.g., Barnston et al., 2012; Kirtman et al., 2014; Palmer & Anderson, 1994). A main limitation for longer-lead ENSO forecasts arises from subseasonal wind variations such as Westerly Wind Events (WWEs), which play an important role in ENSO evolution (e.g., Lengaigne et al., 2013) but are not predictable beyond an ~2-week lead time (Puy et al., 2017). As a result, forecasting ENSO events beyond 2–3 seasons lead time remains a challenge (Barnston et al., 2012).

The lead relation between the oceanic heat content and ENSO has been conceptualized in the *recharge-discharge oscillator* theory (Jin, 1997a). In this paradigm, easterly wind anomalies induce a slow equatorial Pacific heat content recharge through meridional Sverdrup transport during La Niña. The resulting enhanced heat content favors the development of positive SSTAs through the thermocline feedback, and then an El Niño

through the Bjerknes feedback (Bjerknes, 1969), a positive feedback loop between the ocean and atmosphere. The resulting westerlies induce an equatorial ocean heat content discharge, thus yielding a cyclic sequence (Jin, 1997a, 1997b), with subseasonal wind forcing contributing to irregularities in the phase transitions (e.g., Jin et al., 2007).

The most widely used index of the long-term recharge described by the recharge oscillator is the *warm water volume* (WWV, volume of water warmer than 20 °C within 120°E to 80°W, 5°S to 5°N), introduced by Meinen and McPhaden (2000). Several studies have however recently underlined that the WWV has relatively fast timescales (McGregor et al., 2016; Neske & McGregor, 2018) and may not be the best proxy of the long-term recharge (Izumo et al., 2018). The seminal studies of Wyrtki (1985) and Jin (1997a) actually underlined the predictive role of the heat content in the western equatorial Pacific (WWV_w; i.e., as WWV but within 120°E to 155°W, 5°S to 5°N) rather than across the entire equatorial Pacific (i.e., WWV). Recent studies have also renewed interest in WWV_w by showing that ENSO events tend to be preceded by anomalous ocean heat content anomalies in the western equatorial Pacific up to 1.5 years before the event (Ballester et al., 2016; Izumo et al., 2018; Larson & Kirtman, 2017; Petrova et al., 2017; Ramesh & Murtugudde, 2013).

The equatorial Pacific heat content (and in particular WWV_w) hence provides a long-lead ENSO predictor. The potential asymmetry of this lead relation between warm and cold ENSO phases has however so far not been explored in detail. The recharge oscillator theory and WWV-based ENSO statistical forecasts (e.g., Clarke & Van Gorder, 2003; Dayan et al., 2014; Izumo et al., 2010; McPhaden, Zhang, et al., 2006) are indeed essentially linear and do not account for El Niño/La Niña asymmetries. Yet El Niño and La Niña exhibit asymmetrical features. El Niño can reach larger amplitudes than La Niña (e.g., Hoerling et al., 1997) but La Niña generally lasts longer (e.g., Okumura & Deser, 2010). ENSO phase transitions are also asymmetrical with El Niño often followed by La Niña, while La Niña is less frequently followed by El Niño (e.g., Kessler, 2002; Larkin & Harrison, 2002). Such asymmetrical features impact ENSO predictability: The more frequent El Niño to La Niña transitions boost long-lead La Niña predictability (DiNezio, Deser, Karspeck, et al., 2017; DiNezio, Deser, Okumura, et al., 2017), while the erratic La Niña to El Niño transitions and enhanced stochastic atmospheric forcing during El Niño may limit its predictability (Chen et al., 2015; Lengaigne et al., 2013; Luo et al., 2008; Menkes et al., 2014; Puy et al., 2017).

In this paper, we explore the asymmetry in the lead relation between oceanic heat content and ENSO and suggest plausible physical processes behind this asymmetry. The modest length (~40 years) of reliable equatorial Pacific heat content observations is a strong limitation for assessing their lead relation to ENSO. We therefore complement observations with simulations from the Coupled Model Intercomparison Project Phase 5 (CMIP5; Taylor et al., 2012) to allow a more robust statistical assessment of these asymmetries. This paper confirms that WWV_w is the best oceanic heat content predictor of ENSO more than 1 year before its peak but reveals a much stronger relation between a discharged WWV_w and an upcoming La Niña than between a recharged WWV_w and an upcoming El Niño. We finally propose several mechanisms that may contribute to this asymmetry.

2. Methods

WWV indices used in this study are derived from the Bureau of Meteorology Research Center tropical Pacific subsurface temperature data set (Smith, 1995). SST and zonal wind stress are extracted from TropFlux (Praveen Kumar et al., 2012), while precipitations are extracted from GPCPv2.3 (Adler et al., 2003). These monthly data sets are analyzed over the 1980–2016 period.

To complement these short observational data sets, we also analyze multicentennial CMIP5 preindustrial control simulations (r1i1p1 member). As ENSO performance varies among models (e.g., Bellenger et al., 2014), we select the 11 *best* models (out of the 41 available, Table S1) based on two criteria: ENSO seasonality and the ability to simulate extreme El Niño events. Capturing ENSO seasonality is a prerequisite to model the spring predictability barrier: We only select models that exhibit an ENSO peak during boreal winter (see Figures S1a and S1b). We further ensure that the selected models simulate strong El Niño events by retaining models with a rainfall skewness larger than 1 in the eastern Pacific (see Figures S1c and S1d and accompanying text for details; Cai et al., 2014). The selected models accurately reproduce the typical evolution of both ENSO phases, including their main nonlinear features (Figure S2).

For each data sets, interannual anomalies are computed by removing the mean monthly annual cycle and normalized by its monthly standard deviation. All analyses from CMIP5 are performed on the multimodel ensemble (MME), with all models (time series of normalized interannual anomalies) concatenated into a single data set.

ENSO events are defined based on November–January (NDJ) Niño3 (150°W to 90°W, 5°S to 5°N) normalized SSTAs below −0.5 (La Niña), between −0.5 and 0.5 (neutral) and above 0.5 (El Niño). Extreme events are further defined when this index is larger/less than 1.5/−1.5. The same criteria are applied on normalized WWV_w anomalies to define recharged/discharged oceanic states or extreme recharges/discharges.

We estimate the coupling between wind stress and SSTAs (atmospheric component of the Bjerknes feedback) as the regression coefficient of Niño3.4 (170°W to 120°W, 5°S to 5°N) zonal wind stress anomalies onto Niño3 SSTAs, from July to December, when the air-sea coupling is the strongest (Wengel et al., 2018; Zebiak & Cane, 1987). Similarly, regressing precipitation anomalies onto SSTAs provides an estimate of the diabatic heating by deep atmospheric convection (i.e., the driving force of wind stress anomalies).

Statistical significance is estimated through a nonparametric Monte Carlo method throughout the paper. We generate 10,000 random selections of any given sample, with replacement, and provide the 2.5th and 97.5th percentiles of the distribution for the 95% confidence level. The results presented next are robust and do not heavily depend on the details of the methodology described above nor on the model selection procedure (cf. section 4).

3. Asymmetries in the WWV_w/ENSO Lead Relation

CMIP5 MME and observations display very similar lead correlations between WWV indices and ENSO (Figures 1a and 1b): Figures 1a and 1b show that WWV is the best predictor of the upcoming ENSO ($r \sim 0.55$) only in late winter/early spring (January to April). This confirms that WWV is not the best long-term ENSO predictor (Izumo et al., 2018; Meinen & McPhaden, 2000). WWV_w is indeed the best oceanic predictor at long lead times (>1 year) with a maximum correlation around 0.45 during the previous boreal fall, before the winter persistence barrier for WWV (McPhaden, 2003). During this period, the WWV_w region encompasses well the maximum correlation region between the oceanic heat content and Niño3 SSTAs 13 months later (Figure S3). At shorter lead times, after the *spring predictability barrier* (Webster & Yang, 1992), WWV_e (i.e., the eastern Pacific heat content) or typical ENSO indices such as Niño3 SSTAs outperform WWV. There are few discrepancies between CMIP5 and observations, including an earlier maximum lag correlation between WWV_w and ENSO in observations (August–October, 1 year before the event; ASO_{-1}) than in CMIP5 (October–December, 1 year before the event; OND_{-1}). This difference is however well within uncertainties related to the short observational record (black whiskers on Figure 1a). Individual models display some differences in the exact timing and duration of the maximum lead correlation (not shown), but these differences also remain within observational uncertainties. Furthermore, all selected models indicate that WWV_w is the best predictor beyond 1-year lead. WWV_w is thus a robust ENSO predictor more than 1 year before its peak, in both observations and CMIP5.

We now investigate potential asymmetries in the WWV_w/ENSO lead relation. Figures 1c and 1d display a scatterplot between OND_{-1} WWV_w and the NDJ_0 Niño3 SSTAs (13 months later) in observations and CMIP5. Observations suggest a clear asymmetry in this relationship (Figure 1c): Recharged states ($WWV_w > 0.5$) in many instances lead to either a near-neutral state or an El Niño, while discharged states mostly lead to a La Niña. This can be quantified through the slope of the linear regression, which is considerably steeper when considering only La Niña (1.82) rather than only El Niño (0.24). The correlation between WWV_w and ENSO is also different between La Niña (0.46) and El Niño (0.30). This suggests that WWV_w is a better predictor of the amplitude of La Niña than that of El Niño. Because of the short observational record, the uncertainties on these statistics are however large: La Niña slope (correlation) is only larger at the 90% (60%) confidence level. Computing the regressions the other way around (i.e., SSTA as a function of WWV_w) or using one-side regressions leads to the same conclusions, with higher correlation and steeper slope for discharges than for recharges (not shown).

The CMIP5 MME qualitatively reproduces this observed asymmetry (Figures 1c and 1d) but with weaker slopes (0.87 for La Niña and 0.11 for El Niño). While these slopes are both smaller than in observations,

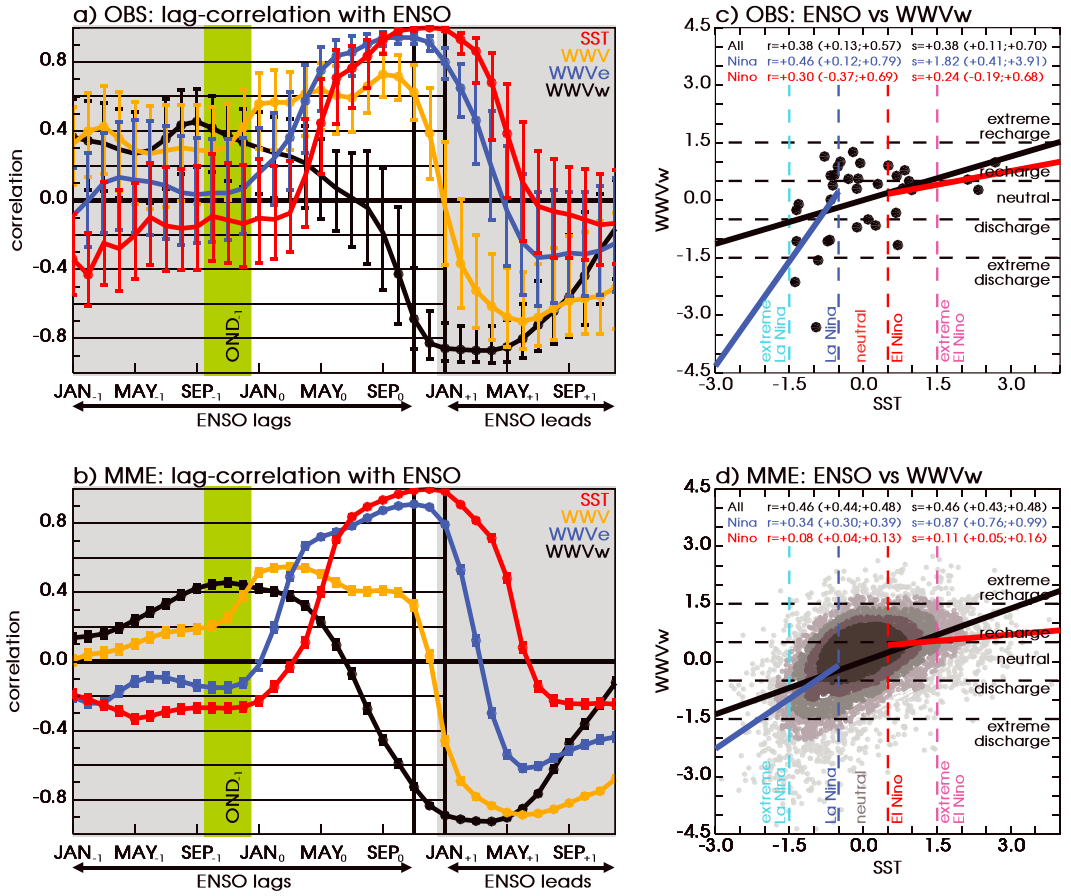

Figure 1. (a, b) Lag correlation between Niño3 (150°W to 90°W, 5°S to 5°N) SST (in red), WWV (in orange; 120°E to 80°W, 5°S to 5°N), WWV_e (in blue; 155°W to 80°W, 5°S to 5°N) and WWV_w (in black; 120°E to 155°W, 5°S to 5°N), and ENSO amplitude at its peak (defined as the November–January average Niño3 SST). Dots and whiskers indicate respectively if the correlation is significantly different from 0 and the confidence interval (both at the 95% level). (c, d) Scatterplot between ENSO amplitude at its peak against WWV_w 13 months before (during OND_{-1}, the shaded green vertical bar in a and b). Black, blue and red solid lines respectively represent the linear regression slopes computed using all values, La Niña events, El Niño events. The corresponding correlation (*r*) and regression slope (*s*) are indicated at the top of each panel, with the 95% confidence interval in brackets. Panels (a) and (c) are computed using observations and (b) and (d), using the MME from 11 selected Coupled Model Intercomparison Project Phase 5 piControl experiments (see text for details). ENSO = El Niño–Southern Oscillation; MME = multimodel ensemble; SST = sea surface temperature; WWV = warm water volume; WWV_e = eastern WWV; WWV_w = western WWV.

their ratio is similar (~8 times larger slope for La Niña). Moreover, CMIP5 slopes lie within the observed slopes confidence intervals (0.4 to 3.9 for La Niña and −0.2 to 0.7 for El Niño). The correlation is also higher for La Niña (0.34) than for El Niño (0.08), and within observational uncertainties (0.1 to 0.8 for La Niña and −0.4 to 0.7 for El Niño). The much larger sample in CMIP5 (more than 5,500 years versus 37 years in observations) yields considerably smaller confidence intervals: The slope and correlation are significantly larger for La Niña than for El Niño at the 99% confidence level. This stronger relation between WWV_w and La Niña amplitudes occurs in all selected CMIP5 models but one (Figure S4). The correlation and slope for each model are within observational uncertainties except for El Niño in one model (Figure S4). Overall, the stronger link between OND_{-1} WWV_w and La Niña amplitudes 13 months later suggested by observations is robust in CMIP5 MME and in virtually every selected CMIP5 model.

Beyond this asymmetry in amplitude, we now investigate if there is a similar asymmetry in the link between WWV_w and the probability of El Niño/La Niña occurrence. In observations, 60% of discharged WWV_w are followed by La Niña 13 months later, 30% by neutral states, and 10% by El Niño. In contrast, there are as many neutral and El Niño (36% each) and 18% La Niña 13 months after a recharged WWV_w, that is, a La Niña is much

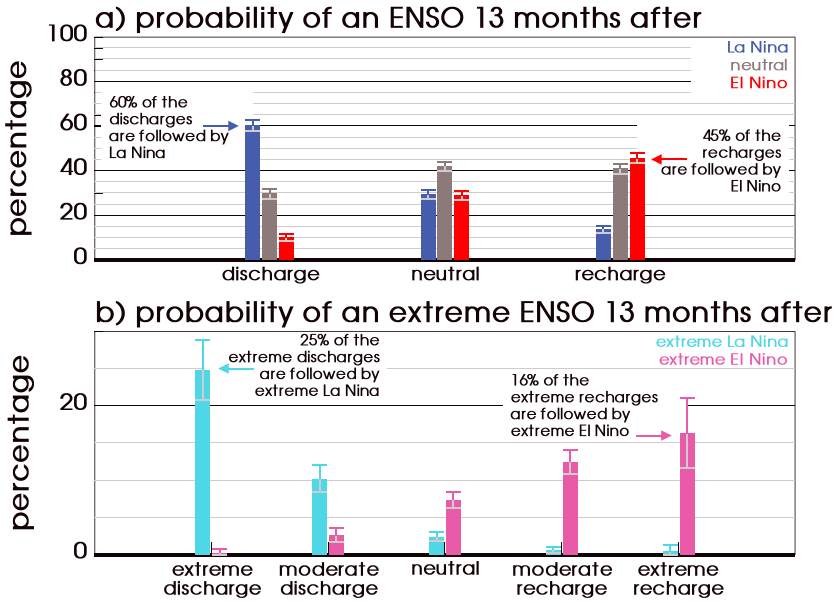

Figure 2. Probability of occurrence of (a) ENSO events and (b) extreme El Niño/La Niña events as a function of the recharge/discharge categories (defined using the warm water volume in the west during October–December, 1 year before the event, 13 months before the ENSO peak), computed using the multimodel ensemble. Whiskers indicate the 95% level confidence interval. ENSO = El Niño–Southern Oscillation.

more likely 1 year after a discharged western Pacific heat content in boreal fall than an El Niño after a recharged heat content. Observations however only cover a short period. In the much larger CMIP5 sample, discharged WWV_w also clearly favor the occurrence of La Niña 1 year later (Figure 2a). As for observations, 60% of the discharges are followed by La Niña, 30% by neutral events, and 10% by El Niño. In contrast, recharges are followed by a similar proportion of El Niño and neutral events (45% and 41%, respectively). This asymmetry is present in every selected model (not shown) and when using all the CMIP5 database (Figure S5). This analysis hence demonstrates that discharged WWV_w is a better predictor of La Niña occurrence than recharged WWV_w of El Niño occurrence.

Finally, the analysis above is repeated specifically for extreme El Niño and La Niña events. With only three extreme El Niño and no extreme la Niña, it is not possible to compute occurrence probabilities in observations. In the larger CMIP5 data set, the occurrence rate of extreme El Niño and La Niña can be computed based on five categories of OND_{-1} WWV_w (extremely discharged, discharged, neutral, recharged, and extremely recharged, Figure 2b—see section 2). In models, the occurrence rate of extreme El Niño/La Niña increases with the level of recharge/discharge. There is however also an asymmetric behavior. Whereas the probability of an extreme El Niño increases gradually (almost linearly) with the recharge level, with 16% of the extreme recharges leading to an extreme El Niño, the probability of an extreme La Niña increases more steeply with the discharge level, with 25% of the extreme discharges leading to an extreme La Niña. This asymmetry, with strongly discharged boreal fall WWV_w leading more systematically to extreme La Niña 13 months later, occurs in each selected CMIP5 models (not shown) and is also present when using all the CMIP5 database (Figure S5).

Using observations and CMIP5 simulations, we have shown that, while positive/negative OND_{-1} WWV_w anomalies are not necessary conditions for the occurrence of El Niño/La Niña 13 months later (as already mentioned by Takahashi & Dewitte, 2016), an early discharged heat content is a better predictor of La Niña occurrence and amplitude than a recharged heat content for that of El Niño.

4. Proposed Mechanism to Explain the WWV_w/ENSO Asymmetry

To explain this asymmetry, we identify two types of mechanisms: the asymmetry in the recharge itself, and the asymmetry in the coupled ocean-atmosphere system stability (i.e., Bjerknes feedback). Below, we focus

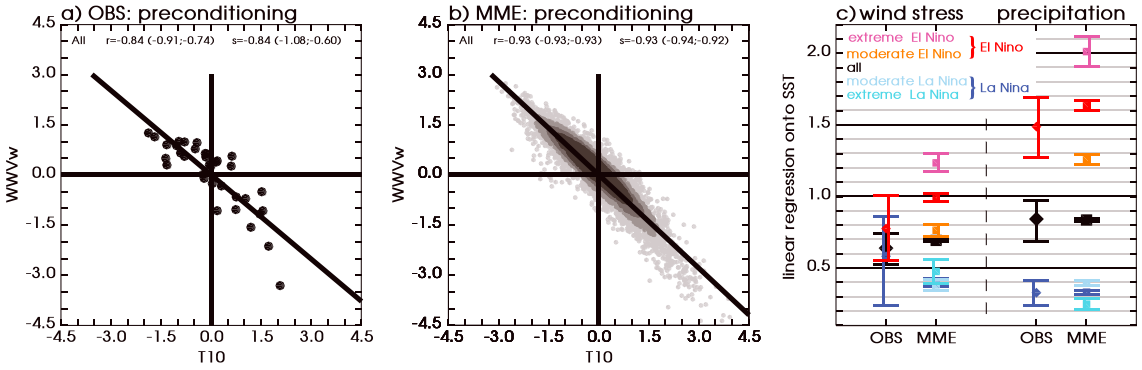

Figure 3. (a, b) Scatterplots between warm water volume in the west in October–December and the integral of zonal wind stress anomalies in equatorial Pacific (120°E to 80°W, 5°S to 5°N) over the previous 10 months (τ_{10}) in (a) observations and (b) the MME. The black solid line represents the linear regression slope. The correlation (*r*) and regression slope (*s*) are indicated at the top of each panel, with the 95% confidence interval in brackets. (c) Linear regression slopes of zonal wind stress and precipitation (both averaged in Niño3.4; 170°W to 120°W, 5°S to 5°N) onto Niño3 SST, computed over the July to December period from observations (diamonds) and the MME (squares). Those are proxies of the zonal wind stress and convective responses to SST variations, forming the atmospheric branch of the Bjerknes feedback. Whiskers indicate the 95% level confidence interval.

on diagnosing the Bjerknes feedback at the seasonal timescale, due to the unavailability of high-frequency outputs for most CMIP5 model. We however come back to the potential role of WWEs in the discussion and illustrate it based on one CMIP5 model.

We first explore the potential role of OND_{-1} WWV_w skewed distribution and its causes. WWV_w distribution is negatively skewed in both observations and CMIP5 (Figure 1c and 1d; −1.31 and −0.64, respectively), that is, boreal fall WWV_w discharges can reach larger amplitudes than recharges. While this skewed WWV_w distribution cannot explain the amplitude predictability asymmetry, that is, the difference in slopes between El Niño and La Niña, it can partly explain the difference in the WWV_w/ENSO correlation between El Niño and La Niña. Larger discharge amplitudes indeed yield a more favorable signal-to-noise ratio for La Niña than for El Niño amplitude. We now investigate the causes of this asymmetric WWV_w distribution. Izumo et al. (2018) demonstrated that WWV_w variations are mainly controlled by wind-forced Rossby waves and can therefore be approximated by the opposite of equatorial Pacific average (i.e., 5°N to 5°S) zonal wind stress anomalies, integrated over last 10 months (hereafter τ_{10}). Figures 3a and 3b display a scatterplot of this wind stress-based proxy against OND WWV_w distribution, in observations and CMIP5 MME, respectively. The wind stress-based proxy explains WWV_w quite well in both observations ($r = 0.84$) and in CMIP5 ($r = 0.93$). Figures 3a and 3b also show that positive τ_{10} can be 30% larger than negative ones in CMIP5, that is, that WWV_w skewness can be partly explained by the τ_{10} skewness (−0.15 in observations, −0.25 in CMIP5). This τ_{10} skewness is itself related to asymmetrical wind stress anomalies, related to larger zonal wind stress anomalies during El Niño (Figure S2). The occurrence of larger zonal wind stress anomalies during El Niño is itself related to two asymmetrical features: (i) the skewed distribution of ENSO, with El Niño that can reach a larger amplitude than La Niña (e.g., Hoerling et al., 1997) and/or (ii) the nonlinearity of the wind stress response: A given surface temperature anomaly yields a larger westerly anomaly during El Niño than easterly anomaly during La Niña, in relation with the nonlinearity of deep atmospheric convection (Choi et al., 2013; Takahashi & Dewitte, 2016).

As ENSO events grow due to the positive Bjerknes feedback, asymmetries in the WWV_w/ENSO predictive relation may be related to asymmetries in this Bjerknes feedback. Figure 3c displays proxies of the atmospheric component of the seasonal Bjerknes feedback during boreal summer and fall (cf. section 2), computed separately for La Niña and El Niño. In observations and CMIP5, this proxy is larger during El Niño (0.8 and 1.0, respectively) than during La Niña (0.6 and 0.4, respectively). This nonlinear behavior of the Bjerknes feedback is even stronger when considering extreme events (which can only be done in CMIP5; Figure 3c). This nonlinearity in the wind stress response can itself be related to the nonlinearity in the deep atmospheric convection (and precipitation) response to SSTAs (Figure 3c), already mentioned by previous studies (Takahashi & Dewitte, 2016; Zheng et al., 2014). The ~28 °C threshold for deep atmospheric convection to occur (e.g., Graham & Barnett, 1987) indeed implies a stronger deep atmospheric convective response to SSTAs during El Niño in both the MME and observations (Figure 3c) and hence a larger

tropospheric heating and stronger near-surface wind response. This asymmetry in the Bjerknes feedback could explain part of the asymmetrical WWV_w/ENSO relation: A stronger feedback implies (1) a more asymmetric τ_{10} and thus WWV_w (2) a more unstable state and hence a stronger growth of errors for instance associated with the unpredictable subseasonal wind variations (e.g., Puy et al., 2017). In the case of La Niña, the less unstable state yields a weaker error growth and hence a more predominant effect of the oceanic preconditioning.

5. Discussion

Our results show that boreal fall WWV_w discharge is a better long-lead predictor of the occurrence and amplitude of La Niña ~1 year later than its recharge for El Niño. This is reminiscent of Luo et al. (2008), who demonstrated that a dynamical model was able to accurately predict the peak phases of the past two long-lasting La Niña up to 2 years in advance, while the 1997 El Niño could not be predicted at such a long lead time. Along the same lines, Gonzalez and Goddard (2016) analyzed CMIP5 decadal prediction experiments and showed that the probabilistic skill for event detection at 1- to 2-year lead is larger for La Niña than for El Niño. Analyzing ensembles from a single coupled model initialized in March, Larson and Kirtman (2017) also found more ensemble spread in forecasts initialized with a recharged state than in those from a discharged state. This is consistent with our interpretation that La Niña is more predictable than El Niño. They however point out that, despite the larger spread, the larger amplitude of El Niño yields a more favorable signal-to-noise ratio. While this differ from our interpretation, the mismatch may come from the fact that they consider symmetric recharged and discharged states, while CMIP5 and observations indicate a clear asymmetry, with larger discharges (Figures 1c and 1d). Timmermann et al. (2018) suggested that the occurrence of El Niño is more predictable than that of La Niña at long lead time (before the spring predictability barrier) in the North American multimodel ensemble (Barnston et al., 2017). They deduced this from the broader distribution of WWV_w anomalies before La Niña than before El Niño. We also find a broader WWV_w distribution at ~1-year lead ahead of La Niña events in both models and observations (Figures 1c, 1d, S6a, and S6b) but disagree with their interpretation on predictability. This broader distribution is indeed the consequence of the fact that some recharged states can lead to La Niña events, that is, that there is a broader range of outcomes after a recharged (Niño, neutral, and some Niña) than after a discharged states (mostly Niña and some neutral), as clearly shown by Figure 2. In other words, discharged WWV_w increase La Niña likelihood more than recharged states increase El Niño likelihood.

Our results are very robust irrespective of methodological choices, for example, detrending time series or not, normalizing anomalies or not, or small variations of the thresholds used to define ENSO and WWV_w categories (not shown). Computing our diagnostics using WWV_w at other seasons (JAS_{-1}, DJF_0), using DJF_0 or MAM_0 WWV (when it is the best predictor of ENSO) yields similar asymmetries in WWV_w/ENSO and WWV/ENSO relationships. Finally, the WWV_w/ENSO asymmetry is weakly sensitive to the model selection and remains significant when applying our diagnostics to the entire CMIP5 database (41 models; Figure S5). The stronger WWV_w/La Niña relation is significant at the 95% confidence level in 28 models out of 41, and no model displays a significantly stronger WWV_w/El Niño relation (Figure S4).

Some ENSO asymmetrical features may partly explain the more robust La Niña long-lead oceanic predictors. La Niña can last 2 years, while it is very rarely the case for El Niño. To test the influence of this asymmetry, we recomputed La Niña minus El Niño linear regression slopes, removing the long-lasting (more than 1 year) La Niña from our statistics (Figure S7). This reduces the slope difference by 22% but the WWV_w/La Niña relation still remains stronger. Long-lasting La Niña events (which frequently follow an extreme El Niño) hence increase La Niña predictability as previously suggested by DiNezio, Deser, Karspeck, et al. (2017) and DiNezio, Deser, Okumura, et al. (2017) but are not the sole source of this increased predictability. ENSO phase transitions are also asymmetrical with El Niño more often followed by La Niña than the opposite (e.g., Kessler, 2002; Larkin & Harrison, 2002). Removing the El Niño to La Niña transitions also yields a 32% reduction of the slope difference but does not suppress it. The fact that extreme El Niño can reach larger amplitudes than extreme La Niña (e.g., Hoerling et al., 1997) does not impact significantly the WWV_w/ENSO asymmetry. On the other hand, extreme discharges of the western equatorial Pacific are by themselves responsible of half of the WWV_w/ENSO asymmetry. The skewness of the WWV_w distribution is therefore fundamental for this asymmetry.

One of the mechanisms that could explain the stronger La Niña predictability is a weaker seasonal Bjerknes feedback. However, the Bjerknes feedback also has a subseasonal component: WWEs occur more frequently when the western Pacific warm pool is abnormally shifted to the east, that is, during El Niño (Eisenman et al., 2005; Lengaigne et al., 2003; Puy et al., 2016; Seiki & Takayabu, 2007). Despite this deterministic control, Puy et al. (2017) demonstrated that WWEs have a sufficiently strong stochastic component to yield a weak El Niño (as observed in 2014) or strong event (as observed in 2015) starting from the same recharged initial state in boreal fall. This stochastic component of WWEs hence contributes to blur El Niño predictability, even in presence of a strong initial recharge, while the less-frequent WWEs may boost predictability during La Niña. The lack of daily data for most CMIP5 piControl experiments prevented us from systematically exploring the impact of WWEs on the predictability of El Niño versus La Niña. In the CNRM-CM5 model, for which daily outputs are available to us, we can however verify that WWEs occur more frequently and can reach larger amplitudes during El Niño (see Figure S8). In addition, the broad WWEs distribution during El Niño highlight that WWEs can have very different value for a given El Niño amplitude that may lead to a weaker El Niño predictability.

The picture emerging from the current work, and that of others, is that ENSO predictability results from a competition between the processes through which the long-term oceanic heat content generates SSTAs and the atmospheric nonlinearities (at both seasonal and subseasonal timescales). For La Niña, the larger amplitude of discharged states yields a stronger effect on SST (i.e., more signal), while the less unstable ocean-atmosphere system yields less error growth (i.e., less noise). The more unstable and more stochastic atmosphere plays a larger role for El Niño. In the near future, we will explore the mechanisms behind this competition using dedicated model experiments.

Acknowledgments

Eric Guilyardi is funded by the Centre National de la Recherche Scientifique (CNRS) and from the National Centre for Atmospheric Science, a UK Natural Environment Research Council collaborative centre. Takeshi Izumo, Matthieu Lengaigne, and Jérome Vialard are funded by Institut de Recherche pour le Développement (IRD). Yann Planton is funded by the Belmont project GOTHAM, under grant ANR-15-JCLI-0004-01. For CMIP the U.S. Department of Energy's Program for Climate Model Diagnosis and Intercomparison provided the coordinating support and led development of software infrastructure in partnership with the Global Organization for Earth System Science Portals. CMIP5 data can be accessed at https://esgf-node.llnl.gov/projects/cmip5/. GODAS and GPCP data are provided by the NOAA/OAR/ESRL PSD, Boulder, Colorado, USA, from their Web site at https://www.esrl.noaa.gov/psd/. The WWV data provided by TAO Project Office of NOAA/PMEL can be downloaded from their Web site: https://www.pmel.noaa.gov/elnino/upper-ocean-heat-content-and-enso. The TropFlux data are produced under a collaboration between Laboratoire d'Océanographie: Expérimentation et Approches Numériques (LOCEAN) from Institut Pierre Simon Laplace (IPSL, Paris, France) and National Institute of Oceanography/CSIR (NIO, Goa, India) and supported by Institut de Recherche pour le Développement (IRD, France). TropFlux relies on data provided by the ECMWF Re-Analysis interim (ERA-I) and ISCCP projects. TropFlux data can be downloaded from http://www.incois.gov.in/tropflux/overview.jsp.

References

Adler, R. F., Huffman, G. J., Chang, A., Ferraro, R., Xie, P.-P., Janowiak, J., et al. (2003). The version-2 Global Precipitation Climatology Project (GPCP) monthly precipitation analysis (1979–present). *Journal of Hydrometeorology*, *4*(6), 1147–1167. https://doi.org/10.1175/1525-7541(2003)004<1147:TVGPCP>2.0.CO;2

Ballester, J., Petrova, D., Bordoni, S., Cash, B., García-Díez, M., & Rodó, X. (2016). Sensitivity of El Niño intensity and timing to preceding subsurface heat magnitude. *Scientific Reports*, *6*(1), 36,344. https://doi.org/10.1038/srep36344

Barnston, A. G., Tippett, M. K., L'Heureux, M. L., Li, S., & DeWitt, D. G. (2012). Skill of real-time seasonal ENSO model predictions during 2002–11: Is our capability increasing? *Bulletin of the American Meteorological Society*, *93*(5), 631–651. https://doi.org/10.1175/BAMS-D-11-00111.1

Barnston, A. G., Tippett, M. K., Ranganathan, M., & L'Heureux, M. L. (2017). Deterministic skill of ENSO predictions from the North American multimodel ensemble. *Climate Dynamics*. https://doi.org/10.1007/s00382-017-3603-3

Bellenger, H., Guilyardi, E., Leloup, J., Lengaigne, M., & Vialard, J. (2014). ENSO representation in climate models: From CMIP3 to CMIP5. *Climate Dynamics*, *42*(7-8), 1999–2018. https://doi.org/10.1007/s00382-013-1783-z

Bjerknes, J. (1969). Atmospheric teleconnections from the equatorial Pacific. *Monthly Weather Review*, *97*(3), 163–172. https://doi.org/10.1175/1520-0493(1969)097<0163:ATFTEP>2.3.CO;2

Bulmer, M. G. (1979). *Principles of statistics*. New York: Dover Publication, INC.

Cai, W., Borlace, S., Lengaigne, M., van Rensch, P., Collins, M., Vecchi, G., et al. (2014). Increasing frequency of extreme El Niño events due to greenhouse warming. *Nature Climate Change*, *4*(2), 111–116. https://doi.org/10.1038/nclimate2100

Chen, D., Lian, T., Fu, C., Cane, M. A., Tang, Y., Murtugudde, R., et al. (2015). Strong influence of westerly wind bursts on El Niño diversity. *Nature Geoscience*, *8*(5), 339–345. https://doi.org/10.1038/ngeo2399

Choi, K.-Y., Vecchi, G. A., & Wittenberg, A. T. (2013). ENSO transition, duration, and amplitude asymmetries: Role of the nonlinear wind stress coupling in a conceptual model. *Journal of Climate*, *26*(23), 9462–9476. https://doi.org/10.1175/JCLI-D-13-00045.1

Clarke, A. J., & Van Gorder, S. (2003). Improving El Niño prediction using a space-time integration of Indo-Pacific winds and equatorial Pacific upper ocean heat content. *Geophysical Research Letters*, *30*(7), 1399. https://doi.org/10.1029/2002GL016673

Dayan, H., Vialard, J., Izumo, T., & Lengaigne, M. (2014). Does sea surface temperature outside the tropical Pacific contribute to enhanced ENSO predictability? *Climate Dynamics*, *43*(5–6), 1311–1325. https://doi.org/10.1007/s00382-013-1946-y

DiNezio, P. N., Deser, C., Karspeck, A., Yeager, S., Okumura, Y., Danabasoglu, G., et al. (2017). A two-year forecast for a 60–80% chance of La Niña in 2017–2018. *Geophysical Research Letters*, *44*, 11,624–11,635. https://doi.org/10.1002/2017GL074904

DiNezio, P. N., Deser, C., Okumura, Y., & Karspeck, A. (2017). Predictability of 2-year La Niña events in a coupled general circulation model. *Climate Dynamics*, *49*(11-12), 4237–4261. https://doi.org/10.1007/s00382-017-3575-3

Eisenman, I., Yu, L., & Tziperman, E. (2005). Westerly wind bursts: ENSO's tail rather than the dog? *Journal of Climate*, *18*(24), 5224–5238. https://doi.org/10.1175/JCLI3588.1

Gonzalez, P. L. M., & Goddard, L. (2016). Long-lead ENSO predictability from CMIP5 decadal hindcasts. *Climate Dynamics*, *46*(9–10), 3127–3147. https://doi.org/10.1007/s00382-015-2757-0

Graham, N. E., & Barnett, T. P. (1987). Sea surface temperature, surface wind divergence, and convection over tropical oceans. *Science*, *238*(4827), 657–659. https://doi.org/10.1126/science.238.4827.657

Hoerling, M. P., Kumar, A., & Zhong, M. (1997). El Niño, La Niña, and the nonlinearity of their teleconnections. *Journal of Climate*, *10*(8), 1769–1786. https://doi.org/10.1175/1520-0442(1997)010<1769:ENOLNA>2.0.CO;2

Hu, Z.-Z., Kumar, A., Huand, B., Zhu, J., Zhang, R.-H., & Jin, F.-F. (2017). Asymmetric evolution of El Niño and La Niña: The recharge/discharge processes and role of the off-equatorial sea surface height anomaly. *Climate Dynamics*, *49*(7-8), 2737–2748. https://doi.org/10.1007/s00382-016-3498-4

Izumo, T., Lengaigne, M., Vialard, J., Suresh, I., & Planton, Y. (2018). On the physical interpretation of the lead relation between the warm water volume and the El Niño Southern Oscillation. *Climate Dynamics*. https://doi.org/10.1007/s00382-018-4313-1

Izumo, T., Vialard, J., Lengaigne, M., de Boyer Montegut, C., Behera, S. K., Luo, J.-J., et al. (2010). Influence of the state of the Indian Ocean dipole on the following year's El Niño. *Nature Geoscience*, *3*(3), 168–172. https://doi.org/10.1038/ngeo760

Jin, F.-F. (1997a). An equatorial ocean recharge paradigm for ENSO. Part I: Conceptual model. *Journal of the Atmospheric Sciences*, *54*(7), 811–829. https://doi.org/10.1175/1520-0469(1997)054<0811:AEORPF>2.0.CO;2

Jin, F.-F. (1997b). An equatorial ocean recharge paradigm for ENSO. Part II: A stripped-down coupled model. *Journal of the Atmospheric Sciences*, *54*(7), 830–847. https://doi.org/10.1175/1520-0469(1997)054<0830:AEORPF>2.0.CO;2

Jin, F.-F., Lin, L., Timmermann, A., & Zhao, J. (2007). Ensemble-mean dynamics of the ENSO recharge oscillator under state-dependent stochastic forcing. *Geophysical Research Letters*, *34*, L03807. https://doi.org/10.1029/2006GL027372

Kessler, W. S. (2002). Is ENSO a cycle or a series of events? *Geophysical Research Letters*, *29*(23), 2125. https://doi.org/10.1029/2002GL015924

Kirtman, B. P., Min, D., Infanti, J. M., Kinter, J. L., Paolino, D. A., Zhang, Q., et al. (2014). The north American multimodel ensemble: Phase-1 seasonal-to-interannual prediction; phase-2 toward developing intraseasonal prediction. *Bulletin of the American Meteorological Society*, *95*(4), 585–601. https://doi.org/10.1175/BAMS-D-12-00050.1

Larkin, N. K., & Harrison, D. E. (2002). ENSO warm (El Niño) and cold (La Niña) event life cycles: Ocean surface anomaly patterns, their symmetries, asymmetries, and implications. *Journal of Climate*, *15*(10), 1118–1140. https://doi.org/10.1175/1520-0442(2002)015<1118:EWENOA>2.0.CO;2

Larson, S. M., & Kirtman, B. P. (2017). Linking preconditioning to extreme ENSO events and reduced ensemble spread. *Climate Dynamics*. https://doi.org/10.1007/s00382-017-3791-x

Lengaigne, M., Boulanger, J.-P., Menkes, C., Delecluse, P., & Slingo, J. (2013). Westerly wind events in the tropical Pacific and their influence on the coupled ocean-atmosphere system: A review. In C. Wang, S. Xie, & J. Carton (Eds.), *Earth's climate: The ocean-atmosphere interaction* (pp. 49–69). Washington, DC: American Geophysical Union. https://doi.org/10.1029/147GM03

Lengaigne, M., Boulanger, J.-P., Menkes, C., Madec, G., Delecluse, P., Guilyardi, E., & Slingo, J. (2003). The March 1997 westerly wind event and the onset of the 1997/98 El Niño: Understanding the role of the atmospheric response. *Journal of Climate*, *16*(20), 3330–3343. https://doi.org/10.1175/1520-0442(2003)016<3330:Tmwwea>2.0.Co;2

Luo, J.-J., Masson, S., Behera, S. K., & Yamagata, T. (2008). Extended ENSO predictions using a fully coupled ocean–atmosphere model. *Journal of Climate*, *21*(1), 84–93. https://doi.org/10.1175/2007JCLI1412.1

McGregor, S., Timmermann, A., Jin, F.-F., & Kessler, W. S. (2016). Charging El Niño with off-equatorial westerly wind events. *Climate Dynamics*, *47*(3-4), 1111–1125. https://doi.org/10.1007/s00382-015-2891-8

McPhaden, M. J. (2003). Tropical Pacific Ocean heat content variations and ENSO persistence barriers. *Geophysical Research Letters*, *30*(9), 1480. https://doi.org/10.1029/2003GL016872

McPhaden, M. J., Zebiak, S. E., & Glantz, M. H. (2006). ENSO as an integrating concept in earth science. *Science*, *314*(5806), 1740–1745. https://doi.org/10.1126/science.1132588

McPhaden, M. J., Zhang, X., Hendon, H. H., & Wheeler, M. C. (2006). Large scale dynamics and MJO forcing of ENSO variability. *Geophysical Research Letters*, *33*, L16702. https://doi.org/10.1029/2006GL026786

Meinen, C. S., & McPhaden, M. J. (2000). Observations of warm water volume changes in the equatorial Pacific and their relationship to El Niño and La Nina. *Journal of Climate*, *13*(20), 3551–3559. https://doi.org/10.1175/1520-0442(2000)013<3551:OOWWVC>2.0.CO;2

Menkes, C. E., Lengaigne, M., Vialard, J., Puy, M., Marchesiello, P., Cravatte, S., & Cambon, G. (2014). About the role of westerly wind events in the possible development of an El Niño in 2014. *Geophysical Research Letters*, *41*, 6476–6483. https://doi.org/10.1002/2014GL061186

Neske, S., & McGregor, S. (2018). Understanding the warm water volume precursor of ENSO events and its interdecadal variation. *Geophysical Research Letters*, *45*, 1577–1585. https://doi.org/10.1002/2017GL076439

Okumura, Y. M., & Deser, C. (2010). Asymmetry in the duration of El Niño and La Niña. *Journal of Climate*, *23*(21), 5826–5843. https://doi.org/10.1175/2010JCLI3592.1

Palmer, T. N., & Anderson, D. L. T. (1994). The prospects for seasonal forecasting—A review paper. *Quarterly Journal of the Royal Meteorological Society*, *120*(518), 755–793. https://doi.org/10.1002/qj.49712051802

Petrova, D., Koopman, S. J., Ballester, J., & Rodó, X. (2017). Improving the long-lead predictability of El Niño using a novel forecasting scheme based on a dynamic components model. *Climate Dynamics*, *48*(3-4), 1249–1276. https://doi.org/10.1007/s00382-016-3139-y

Praveen Kumar, B., Vialard, J., Lengaigne, M., Murty, V. S. N., & McPhaden, M. J. (2012). TropFlux: Air-sea fluxes for the global tropical oceans—Description and evaluation. *Climate Dynamics*, *38*(7-8), 1521–1543. https://doi.org/10.1007/s00382-011-1115-0

Puy, M., Vialard, J., Lengaigne, M., & Guilyardi, E. (2016). Modulation of equatorial Pacific westerly/easterly wind events by the Madden-Julian oscillation and convectively-coupled Rossby waves. *Climate Dynamics*, *46*(7), 2155–2178. https://doi.org/10.1007/s00382-016-3480-1

Puy, M., Vialard, J., Lengaigne, M., Guilyardi, E., DiNezio, P. N., Voldoire, A., et al. (2017). Influence of westerly wind events stochasticity on El Niño amplitude: The case of 2014 vs. 2015. *Climate Dynamics*. https://doi.org/10.1007/s00382-017-3938-9

Ramesh, N., & Murtugudde, R. (2013). All flavours of El Niño have similar early subsurface origins. *Nature Climate Change*, *3*(1), 42–46. https://doi.org/10.1038/nclimate1600

Saha, S., Nadiga, S., Thiaw, C., Wang, J., Wang, W., Zhang, Q., et al. (2006). The NCEP climate forecast system. *Journal of Climate*, *19*(15), 3483–3517. https://doi.org/10.1175/JCLI3812.1

Santoso, A., McPhaden, M. J., & Cai, W. (2017). The defining characteristics of ENSO extremes and the strong 2015/2016 El Niño. *Reviews of Geophysics*, *55*, 1079–1129. https://doi.org/10.1002/2017RG000560

Seiki, A., & Takayabu, Y. N. (2007). Westerly wind bursts and their relationship with intraseasonal variations and ENSO. Part I: Statistics. *Monthly Weather Review*, *135*(10), 3325–3345. https://doi.org/10.1175/MWR3477.1

Smith, N. R. (1995). An improved system for tropical ocean subsurface temperature analyses. *Journal of Atmospheric and Oceanic Technology*, *12*(4), 850–870. https://doi.org/10.1175/1520-0426(1995)012<0850:AISFTO>2.0.CO;2

Takahashi, K., & Dewitte, B. (2016). Strong and moderate nonlinear El Niño regimes. *Climate Dynamics*, *46*(5-6), 1627–1645. https://doi.org/10.1007/s00382-015-2665-3

Taylor, K. E., Stouffer, R. J., & Meehl, G. A. (2012). An overview of CMIP5 and the experiment design. *Bulletin of the American Meteorological Society*, *93*(4), 485–498. https://doi.org/10.1175/BAMS-D-11-00094.1

Timmermann, A., An, S.-I., Kug, J.-S., Jin, F.-F., Cai, W., Capotondi, A., et al. (2018). El Niño-Southern Oscillation complexity. *Nature*, *559*, 535–545. https://doi.org/10.1038/s41586-018-0252-6

Webster, P. J., & Yang, S. (1992). Monsoon and ENSO: Selectively interactive systems. *Quarterly Journal of the Royal Meteorological Society*, *118*(507), 877–926. https://doi.org/10.1002/qj.49711850705

Wengel, C., Latif, M., Park, W., Harlass, J., & Bayr, T. (2018). Seasonal ENSO phase locking in the Kiel climate model: The importance of the equatorial cold sea surface temperature bias. *Climate Dynamics*, *50*(3-4), 901–919. https://doi.org/10.1007/s00382-017-3648-3

Wyrtki, K. (1985). Water displacements in the Pacific and the genesis of El Niño cycles. *Journal of Geophysical Research*, *90*, 7129–7132. https://doi.org/10.1029/JC090iC04p07129

Zebiak, S. E., & Cane, M. A. (1987). A model El Niño Southern Oscillation. *Monthly Weather Review*, *115*(10), 2262–2278. https://doi.org/10.1175/1520-0493(1987)115<2262:AMENO>2.0.CO;2

Zheng, F., Fang, X.-H., Yu, J.-Y., & Zhu, J. (2014). Asymmetry of the Bjerknes positive feedback between the two types of El Niño. *Geophysical Research Letters*, *41*, 7651–7657. https://doi.org/10.1002/2014GL062125